

A Multipoint Flux Approximation Method Based on Harmonic Points (MPFA-H) for the Numerical Solution of the Stokes-Brinkman Equations in Carbonate Petroleum Reservoirs

Pedro H. M. Melo¹, Fernando R. L. Contreras², Darlan K.E. Carvalho¹, Paulo R. M. Lyra¹

¹*Departamento de Engenharia Mecânica – Universidade Federal de Pernambuco
Av. Acadêmico Hélio Ramos s/n, CEP: 50670-901, Pernambuco, Recife, Brazil
pedrohmatos17@gmail.com, darlan.ecarvalho@ufpe.br, paulo.lyra@ufpe.br*

²*Núcleo de Tecnologia, Centro Acadêmico do Agreste, (NT-CAA) - Universidade Federal de Pernambuco
Rodovia BR 104 KM 59 s/n: 55002-970, Caruaru, PE-Brazil
ferlicapac@gmail.com*

Abstract. In this work, our main purpose is to present a cell-centered finite volume scheme for the simulation of fluid flow on carbonate petroleum reservoirs using an unstructured polygonal mesh. The governing equations are solved using two different approaches, a monolithic and segregated, the latter employs the SIMPLEC (Semi-Implicit Method for Pressure Linked Equations-Consistent), where the Stokes Brinkman's equations are discretized using a Multipoint Flux Approximation method based on harmonic points (MPFA-H) that can handle highly heterogeneous and anisotropic media. Furthermore, to assure the coupling between the variables, a modification of the Rhie-Chow's interpolation method given by Zhang et al. [1]. is used. The proposed methods are tested and the differences between these two approaches are discussed.

Keywords: Heterogeneous and Anisotropic Carbonate Reservoirs, Stokes-Brinkman Model, Finite Volume Method, Monolithic Procedure, SIMPLEC

1 Introduction

Carbonate (karst) reservoirs, when compared to clastic reservoirs, are very heterogeneous in terms of rock properties. It is estimated that about 60% of the oil and 40% of natural gas world's reserves can be found on carbonate reservoirs (JOSHI;SINGH,2020).

The presence of fractures, vugs and cavities, interconnected or not, and in multiple scales, can change significantly the fluid flow on carbonate petroleum reservoirs, representing a great challenge for the numerical model and simulation of fluid flows. Carbonate reservoirs are composed of sedimentary rocks that are made primarily of carbonate minerals comprising vugs, caves and fractures of different scales. In this context there are two distinct flow regions where we can assume two different models. On the porous material we can accurately use the Darcy's Law and within the free flow region where we should use the Stokes' equation Krotkiewski et al. [3].

Different strategies are used to handle this problem, such as dual or triple porosities, triple permeability and the so-called Darcy-Stokes model. However, when dealing with the carbonate reservoirs, those strategies can be inadequate due the heterogeneity and complexity media that is associated to the three types of porosities, i.e., matrix, fractures and cavities as these fractures and cavities are generally connected to form a fracture-cavity network and are distributed irregularly throughout the rock varying in size, from the microscopic to the macroscopic level. A alternative approach is to employ the Stokes-Brinkman (S-B) model, Brinkman [4], in which a single equation is used to model the porous media flow and the free flow, which, for incompressible fluid flow in transient regime, read:

$$\rho \frac{\partial \mathbf{u}}{\partial t} - \mathcal{D}\mathbf{u} + \mathcal{B}\mathbf{u} = -\nabla p, \quad (1)$$

In eq. (1), \mathbf{u} , is the velocity vector, p represents the fluid pressure, and ρ denotes the fluid density. The operators, $\mathcal{D} = -\nabla \cdot (\mu \nabla)$ and $\mathcal{B} = \mu \mathbf{K}^{-1}$, are used for notation compactness, and μ is the dynamic fluid viscosity and \mathbf{K} is the absolute rock permeability tensor.

To completely determine the problem described in eq. (1) a proper set of boundary and initial conditions need to be applied, Conceição [5]:

$$p(\mathbf{x}, t) = g_D \text{ in } \Gamma_D, \quad \mathbf{u} \cdot \mathbf{n} = g_N \text{ in } \Gamma_N \quad \mathbf{u}(\mathbf{x}, 0) = \mathbf{u}^0 \quad (2)$$

where Γ_N and Γ_D represent the Neumann and Dirichlet boundaries conditions. The scalar g_N (prescribed flux) is applied at Γ_N and g_D (prescribed pressures) is defined at Γ_D , and \mathbf{u}^0 is the initial velocity distribution.

The Stokes-Brinkman model varies smoothly from Stokes to Darcy's models model, as a functions of smoothly varying parameters throughout the different flow regions, Conceição et al. [6], Krotkiewski et al. [3].

2 Finite Volume Discretization of Stokes Brinkman Equations

The discretization of the domain Ω is made by subdividing it into a series of n_V polygonal control volumes ν . Performing the integration of eq. (1) and the divergence free velocity equation eq. (4) over each finite volume ν , the first order, implicit Euler backward method to approximate the time derivative, we obtain:

$$\int_{\nu} \frac{\rho}{\Delta t} (\mathbf{u}^{n+1} - \mathbf{u}^n) d\Omega - \int_{\nu} \mathcal{D} \mathbf{u}^{n+1} d\Omega + \int_{\nu} \mathcal{B} \mathbf{u}^{n+1} d\Omega = - \int_{\nu} \nabla p^{n+1} d\Omega \quad (3)$$

$$\int_{\nu} \nabla \mathbf{u}^{n+1} d\Omega = 0 \quad (4)$$

In the monolithic approach, by means of a proper discretization method, we solve the system formed by eq. (3) and eq. (4) simultaneously, using some iterative technique, Conceição [5].

On the other hand, by adopting a segregated approach, like the SIMPLEC, Ferziger et al. [7], the momentum equations are solved with a guessed pressure field to obtain an intermediate velocity field. In order to also satisfy the continuity equation, the velocity field must be corrected. Therefore, at the end of the iterative cycle, the velocity field satisfies both, the momentum and mass conservation equation. The predictor step, in which an intermediate velocity field is computed, which are given by eq. (5) and eq. (6).

$$\int_{\nu} \frac{\rho}{\Delta t} (\mathbf{u}^* - \mathbf{u}^n) d\Omega - \int_{\nu} \mathcal{D} \mathbf{u}^* d\Omega + \int_{\nu} \mathcal{B} \mathbf{u}^* d\Omega = - \int_{\nu} \nabla p^n d\Omega \quad (5)$$

$$\int_{\nu} \nabla \left(\frac{\rho V}{\Delta t} + \mathcal{B} V \right)^{-1} \nabla p' d\Omega = \int_{\nu} \frac{\nabla \mathbf{u}^*}{\Delta t} d\Omega \quad (6)$$

The correction step, for both, pressure and velocity, is given by eq. (7)

$$p = p^n + p' \quad \text{and} \quad \mathbf{u} = \mathbf{u}^* - \int_{\nu} \nabla \left(\frac{\rho V}{\Delta t} + \mathcal{B} V \right)^{-1} p' d\Omega \quad (7)$$

where \mathbf{u}^* is an intermediate velocity field that do not necessarily satisfy the divergence free condition, p' is known as the pressure correction and V is the volume of the cell where the procedure is been employed.

It is worth to mention that, to ensure the coupling between the variables, pressure and velocity, and to avoid non-physicals pressure distribution due the collocated arrangement that was used in this work, a variation of the Rhie-Chow interpolation method was employed to estimate the fluxes along the cell faces, Ferziger et al. [7]. It is well known in literature, that the Rhie-Chow interpolation has some drawbacks, such as: pressure oscillation when a small time step is used and dependence on the value of the under relaxation parameter. In order to avoid those problems, we have adopted some modifications adopted in Zhang et al. [1].

2.1 MPFA discretization

A Multipoint Flux Approximation based on harmonic points (MPFA-H) is used to discretize the terms in the Stokes-Brinkman and continuity equations. The MPFA-H is used to spacially discretize the terms $\int_{\nu} \mathcal{D}\phi d\Omega$, the discretization of the term $\int_{\nu} \mathcal{D}\phi d\Omega$ is detailed in Contreras [8] when dealing with classical Darcian flow, therefore, in the present paper, we will restrict our attention to the $\int_{\nu} \nabla p d\Omega$ term.

Discretization of $\int_{\nu} \nabla p d\Omega$

Consider two control volumes, named \hat{R} and \hat{L} , that share a face IJ (edge in 2D), with the respective permeability tensors $\mathbf{K}_{\hat{R}}$ and $\mathbf{K}_{\hat{L}}$ and $x_{\hat{R}}$ and $x_{\hat{L}}$ are the centroids of the control volumes \hat{R} and \hat{L} . The interpolation point over the control surface associated to a face IJ , shared by the two control volumes in question, is defined by Contreras [8]:

$$y_{IJ} = \frac{h_{\hat{L},IJ} \mathbf{K}_{\hat{R},IJ}^{(n)} x_{\hat{R}} + h_{\hat{R},IJ} \mathbf{K}_{\hat{L},IJ}^{(n)} x_{\hat{L}} + h_{\hat{L},IJ} h_{\hat{R},IJ} (\mathbf{K}_{\hat{L}}^{\top} - \mathbf{K}_{\hat{R}}^{\top}) \vec{n}_{IJ}}{h_{\hat{L},IJ} \mathbf{K}_{\hat{R},IJ}^{(n)} + h_{\hat{R},IJ} \mathbf{K}_{\hat{L},IJ}^{(n)}} \quad (8)$$

where y_{IJ} is the as harmonic point, $h_{\hat{R},IJ}$ and $h_{\hat{L},IJ}$ are the orthogonal distances from the centroids of the adjacent control volumes to the face IJ , and $\mathbf{K}_{\hat{R},IJ}^{(n)} = \mathbf{n}_{IJ}^{\top} \mathbf{K}_{\hat{R}} \mathbf{n}_{IJ}$ and $\mathbf{K}_{\hat{L},IJ}^{(n)} = \mathbf{n}_{IJ}^{\top} \mathbf{K}_{\hat{L}} \mathbf{n}_{IJ}$ are the conormal projections of the permeability tensors on the face IJ . For control faces inside de domain, we use eq. (8) to determine the interpolation points, and for the boundary faces we use the mid points of the face IJ .

Once all the interpolation points are computed, the next step is to define the pressures on each harmonic point. To do so, the value of theses pressures are considered a convex combination of the pressures of the control volumes adjacents to the face IJ , as shown ineq. (9):

$$p_{IJ} = w_{\hat{L},IJ} p_{\hat{L}} + w_{\hat{R},IJ} p_{\hat{R}} \quad (9)$$

where $w_{\hat{L},IJ}$ and $w_{\hat{R},IJ}$ are harmonic weights that depend on physical and geometrical parameters and are given by:

$$w_{\hat{L},IJ} = \frac{h_{\hat{R},IJ} \mathbf{K}_{\hat{L},IJ}^{(n)}}{h_{\hat{L},IJ} \mathbf{K}_{\hat{R},IJ}^{(n)} + h_{\hat{R},IJ} \mathbf{K}_{\hat{L},IJ}^{(n)}} \quad \text{and} \quad w_{\hat{R},IJ} = 1 - w_{\hat{L},IJ} \quad (10)$$

With the pressures computed on the interpolation points we employ the Green-Gauss theorem to approximate gradients, considering a finite volume ν , as:

$$\int_{\Omega_{\nu}} \nabla p d\Omega_{\nu} = \int_{\Gamma_{\nu}} p \mathbf{n} d\Gamma_{\nu} = \sum_{i=1}^{n_{faces}} p_i s_i \mathbf{n}_{IJ} \quad (11)$$

In eq. (11) p_i stands for pressures on interpolation points and is given by eq. (9), s_i is the area of the control surface (length in 2D) and \mathbf{n}_{IJ} is the normal outward of the face IJ .

3 Numerical results

3.1 Steady State Flow Through a Channel Filled with Porous Material

This problem was adapted from Conceição [5], to verify the proposed formulation considering the fluid flow in a channel build by two parallel plates with a distance H between the plates. plates. The channel is filled with porous material with isotropic permeability, $\mathbf{K} = k\mathbf{I}$. The fluid is considered incompressible, and the dynamic and the effective viscosities are equal, $\mu_{effective} = \mu$. The analytical solution for this problem is given by:

$$v(y) = \frac{\sinh(\lambda(1 - y))}{\sinh(\lambda)} - \frac{G}{\lambda^2\gamma} \left(\frac{\sinh(\lambda(1 - y)) + \sinh(\lambda y)}{\sinh(\lambda)} \right) \quad (12)$$

where G is the pressure gradient along the channel, γ is the ratio between the effective and dynamic viscosities, in this work considered equal to one, and λ is given by:

$$\lambda = \frac{1}{\sqrt{\gamma}} \sqrt{\left(\frac{H^2}{k} + \frac{1}{\sqrt[4]{\frac{k}{H^2}}} \right)} \quad (13)$$

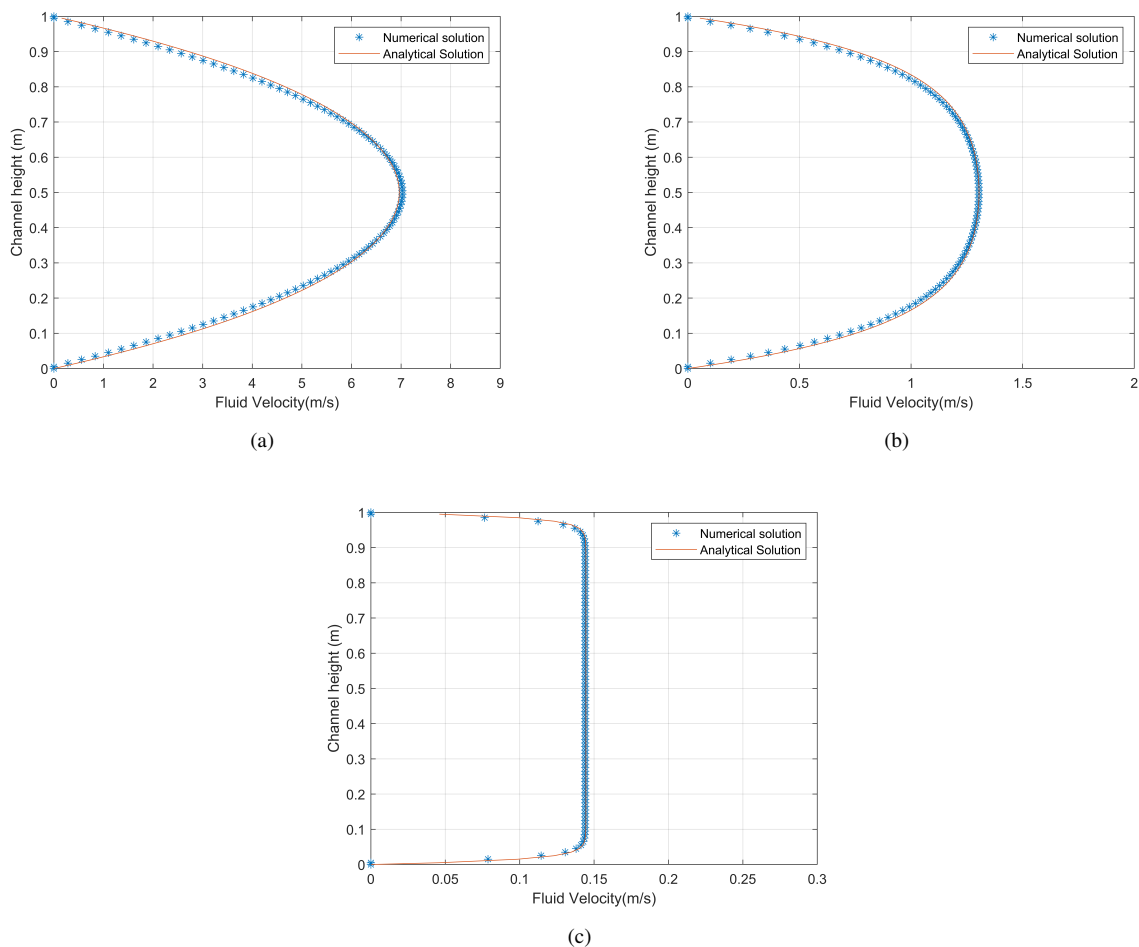


Figure 1. Computational mesh with 100 control volumes and the fluid velocity profiles through the center line for the problem of the flow through a channel filled with porous material for different values of the permeability ; a) $k=1.5 \times 10^{-12} m^2$, b) $k=1.5 \times 10^{-13} m^2$; c) $k=1.5 \times 10^{-15} m^2$.

In this problem we have used a mesh with 100 quadrilateral control volumes. By analysing Fig. 1, it is possible to infer that when the value of permeability decreases, the parabolic profile of the velocities, common in free flows, starts to flatten, representing a Darcy flow. For all cases, we have used the monolithical approach, and, for all different permeability cases we can observe an excellent agreement between the numerical and the analytical solutions.

3.2 Transient Flow in a Channelized Carbonate Karst Domain

In order to compare the different strategies proposed in this paper, initially we define the L2-norm of the error eq. (14) to evaluate the difference in the results of the monolithical and the segregated methods. The values of the reference pressure were taken in a fine scale mesh with 11,766 control volumes using the monolithical approach and p_{method} refers to the pressure obtained with the the different numerical approaches used in this work, monolithical and segregated.

$$\epsilon_p = \left(\frac{\sum_{L \in \Omega} (p_{reference}(x_i) - p_{method}(x_i))}{\sum_{L \in \Omega} (p_{reference}(x_i))} \right)^{\frac{1}{2}} \quad (14)$$

An artificial carbonate karst domain was constructed by adding four karstic formations, represented by ellipses, positioned simetrically along the domain. We considered the rock isotropic matrix permeability, $K = kI$ with $k = 1.5 \times 10^{-15} m^2$, and $k = 1.5 \times 10^{-12} m^2$ in the interior of the vugs. Also the fluid viscosity is equal to 0.7 cP. A pressure drop of 1 psi was imposed along the x direction, and no-flow boundary conditions were imposed on the superior and inferior boundaries. Also, the domain was discretized using a triangular mesh, as it can be seen in Fig. 2.

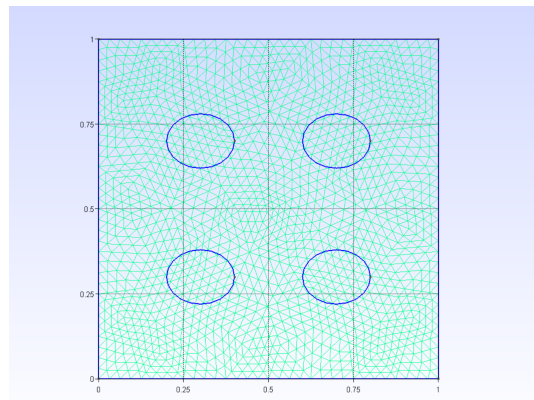


Figure 2. Transient Flow in a Channelized Carbonate Karst Domain: Subregions and triangular mesh with 2,944 control volumes..

The errors and the numerical convergence rates for both, the monolithic and the segregated approaches are presented in Table 1, considering triangular meshes with 184, 736 and 2,944 control volumes. In Fig. 3 we present the pressure drop along the diagonal connecting the bottom left part to the upper right part of the reservoir using the monolithical and the SIMPLEC approaches with a triangular mesh with 2944 control volumes.

For both, monolithical and segregated approach, a mesh convergency analysis was made. The numerical results for both approaches, when 2,944 elements were used, and for the fine scale mesh, along the diagonal direction of the domain can be seen on Fig. 3.

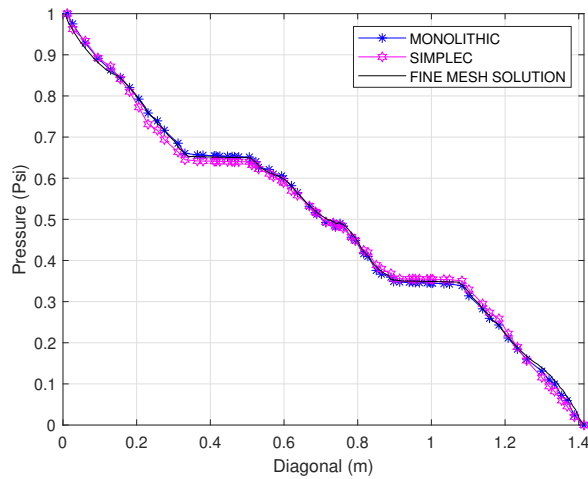


Figure 3. Transient Flow in a Channelized Carbonate Karst Domain: Pressure drop along the diagonal connecting the bottom left part to the upper right part of the reservoir for the triangular mesh with 2944 control volumes using the monolithical and the SIMPLEC approaches.

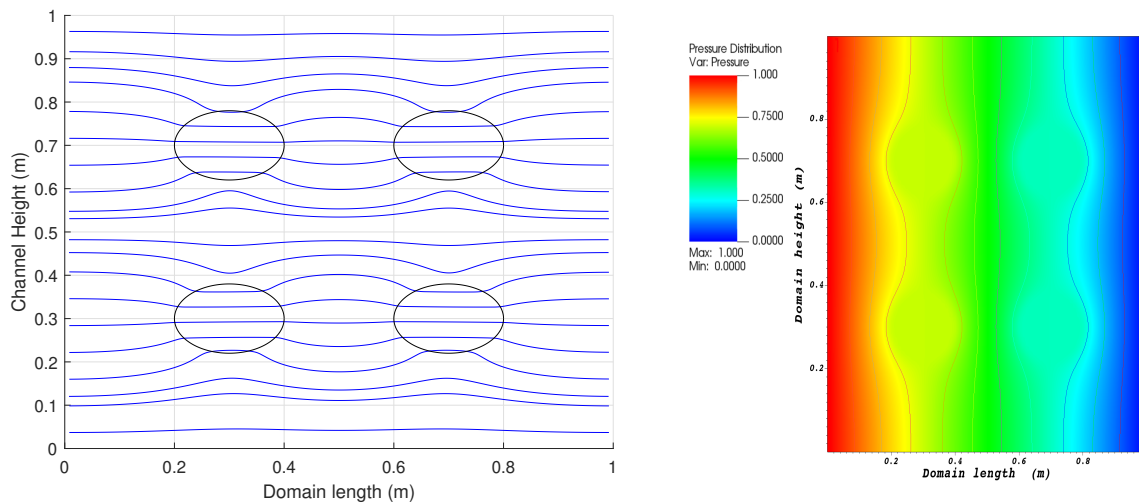


Figure 4. Transient Flow in a Channelized Carbonate Karst Domain: Streamlines (left) and the pressure distribution along the domain (right).

Table 1. Transient Flow in a Channelized Carbonate Karst Domain: Errors and convergence rates for the monolithical and the SIMPLEC approaches..

#CVs		184	736	2944
Monolithical	ϵ_p	0.0953	0.0445	0.0169
	q_{L_2}	–	1.0987	1.3968
SIMPLEC	ϵ_p	0.1041	0.0478	0.0300
	q_{L_2}	–	1.1228	0.6720

In Fig. 3, we present the pressure drop along the diagonal of the channel that connects the lower left part to the upper right part of the reservoir. In this figure, it is clear that the solution of the Stokes-Brinkman model by using using th MPFA-H with both, the monolithical and the SIMPLEC approaches is capable of capturing the porous media (Darcy) and the free flow (Stokes) regions of the carbonate reservoir.

4 Conclusions

In the present paper, we present a cell-centered Multipoint Flux Approximation method based on harmonic points (MPFA-H) to numerically approximate the Stokes-Brinkman equations on heterogeneous porous media using unstructured meshes with a monolithic and a segregated (SIMPLEC) approaches. In addition, a variation of the Rhie-Chow interpolation scheme adapted to unstructured meshes was used to overcome well known issues of this interpolation scheme. The Stokes-Brinkman formulation can depict, without the need to use interface conditions, the fluid flow along the rock matrix and in the free flow regions. In the near future we intend to incorporate compressibility and to extend our formulation for 3D domains.

5 Acknowledgements

The authors would like to thank the Conselho Nacional de Desenvolvimento Científico e Tecnológico – CNPq, Fundação de Amparo à Ciência e Tecnologia do Estado de Pernambuco - FACEPE, Coordenação de Aperfeiçoamento de Pessoal de Nível Superior - CAPES.

Authorship statement. The authors hereby confirm that they are the sole liable persons responsible for the authorship of this work, and that all material that has been herein included as part of the present paper is either the property (and authorship) of the authors, or has the permission of the owners to be included here.

References

- [1] Zhang, S., Zhao, X., & Bayyuk, S., 2014. Generalized formulations for the rhie–chow interpolation. *Journal of Computational Physics*, vol. 258, pp. 880–914.
- [2] Joshi, R. M. & Singh, K. H., 2020. Carbonate reservoirs: Recent large to giant carbonate discoveries around the world and how they are shaping the carbonate reservoir landscape. In *Petro-physics and Rock Physics of Carbonate Reservoirs*, pp. 3–14. Springer.
- [3] Krotkiewski, M., Ligeard, I. S., Lie, K., & Schmid, D. W., 2011. On the importance of the stokes-brinkman equations for computing effective permeability in karst reservoirs. *Communications in Computational Physics*, vol. 10, pp. 1315–1332.
- [4] Brinkman, H. C., 1949. A calculation of the viscous force exerted by a flowing fluid on a dense swarm of particles. *Flow, Turbulence and Combustion*, vol. 1, pp. 27.
- [5] Conceição, S. B., 2019. Simulação numérica de escoamentos em reservatórios carbonáticos utilizando um modelo de Stokes-Brinkman por meio de métodos localmente conservativos. Master's thesis, Universidade Federal de Pernambuco.
- [6] Conceição, S. B., Seidel, M. A., Lyra, P. R. M., & de Carvalho, D. K. E., 2019. Numerical simulation of flows in carbonate reservoirs using a stokes-brinkman model and locally conservative methods. In *Proceedings of the COBEM. 25th ABCM International Congress of Mechanical Engineering*, Uberlândia, MG, Brazil.
- [7] Ferziger, J. H., Milovan, P., & Street, R. L., 1998. *Computational Methods for Fluid Dynamics*. Oxford classic texts in the physical sciences. Clarendon Press.
- [8] Contreras, F. R. L., 2016. A MPFA Method Using Harmonic Points coupled to a Multidimensional Optimal Order Detection Method (mood) for the Simulation of Oil-Water Displacements in Petroleum Reservoirs. In *Revista Interdisciplinar De Pesquisa Em Engenharia*, pp. 76–95, Brasília, Brazil. XXXVII Iberian Latin American Congress on Computational Methods in Engineering.